Nuclear Engineering and Technology 55 (2023) 3150–3163

Contents lists available at ScienceDirect

Nuclear Engineering and Technology

journal homepage: www.elsevier.com/locate/net

Original Article

An intelligent optimization method for the HCSB blanket based on an improved multi-objective NSGA-III algorithm and an adaptive BP neural network

Wen Zhou [a, b, c], Guomin Sun [b, *], Shuichiro Miwa [a], Zihui Yang [b], Zhuang Li [b, c], Di Zhang [b, d], Jianye Wang [b]

[a] Department of Nuclear Engineering and Management, School of Engineering, University of Tokyo, 7-3-1 Hongo, Bunkyo-ku, Tokyo, 113-8654, Japan
[b] Key Laboratory of Neutronics and Radiation Safety, Hefei Institutes of Physical Science, Chinese Academy of Sciences, Hefei, Anhui, 230031, China
[c] University of Science and Technology of China, Hefei, Anhui, 230027, China
[d] Institutes of Physical Science and Information Technology, Anhui University, Hefei, 230601, China

ARTICLE INFO

Article history:
Received 9 January 2023
Accepted 19 May 2023
Available online 26 May 2023

Keywords:
CFETR HCSB blanket
Radial arrangement
Optimization design
NSGA-III algorithm
DE algorithm
BP neural Network

ABSTRACT

To improve the performance of blanket: maximizing the tritium breeding rate (TBR) for tritium self-sufficiency, and minimizing the Dose of backplate for radiation protection, most previous studies are based on manual corrections to adjust the blanket structure to achieve optimization design, but it is difficult to find an optimal structure and tends to be trapped by local optimizations as it involves multi-physics field design, which is also inefficient and time-consuming process. The artificial intelligence (AI) maybe is a potential method for the optimization design of the blanket. So, this paper aims to develop an intelligent optimization method based on an improved multi-objective NSGA-III algorithm and an adaptive BP neural network to solve these problems mentioned above. This method has been applied on optimizing the radial arrangement of a conceptual design of CFETR HCSB blanket. Finally, a series of optimal radial arrangements are obtained under the constraints that the temperature of each component of the blanket does not exceed the limit and the radial length remains unchanged, the efficiency of the blanket optimization design is significantly improved. This study will provide a clue and inspiration for the application of artificial intelligence technology in the optimization design of blanket.

1. Introduction

Fusion energy has the characteristics of "inexhaustibility of resources, intrinsic security, no release of CO2, and no long-lived radioactive wastes," [1], it would be an immense benefit to all mankind and solve the world's energy problems once and for all. The blanket is one of the critical research contents in the process from fusion experimental reactor to fusion demonstration reactor to fusion power plant, which is a significant component that achieves tritium self-sufficiency and converts fusion energy into electricity in fusion reactor [2], accordingly, the design of blanket mainly has three objectives:

1) Maintaining the tritium required for the fusion reactor core for achieving tritium self-sustainability, i.e., tritium breeding ratio (TBR).
2) Transporting the nuclear power deposition and high heat from the plasma through the coolant flowing of internal channels for achieving energy conversion.
3) Providing shielding for protecting the superconducting magnets from neutron radiation.

Therefore, blanket design is a complex multi-objective optimization problem (MOOP) under the multi-physics field (such as neutron, temperature, stress, flow, electromagnetic field, etc.).

The current optimization method of fusion reactor blanket mainly focuses on two types:

The first type is the optimization method based on manual professional experience. The rear manifold, rib, cap, and breeding zone were revised by Wu et al. using multi-physics field analyses with MCNP and ANSYS. The flow diagram of the He coolant and

* Corresponding author.
E-mail address: guomin.sun@inest.cas.cn (G. Sun).

https://doi.org/10.1016/j.net.2023.05.024

purge gas were optimized, which can meet the need for heat removal [3]. According to the research by Hernández et al. [4–6], they ongoing improved the latest design of the Helium Cooled Pebble Bed (HCPB) for the Pre-Conceptual Design (PCD) phase in 2014–2020 based on manual professional experience. The HCPB blanket was optimized to fulfill the TBR, thermal stress stability, and shielding performance by artificial consciousness based on Pereslavtsev's work [7]. The NTCOC software was developed based on a coupled neutronics/thermal optimization code by Zhang [8], it has been used to optimize the radial structure of the Chinese Fusion Engineering Test Reactor (CFETR) helium cooled solid breeder (HCSB) blanket, and the final optimization results were obtained. Although these optimization methods have promoted the progress of blanket design, they still have some limitations that reliance on manual experience, high workload, manual iterative correction between multiple physical fields designs with many variables and a high level of coupling.

The second type is the optimization method based on intelligent algorithm. To find the better structure that can meet the maximum heat flux, the optimization of the first wall (FW) of the water-cooled lithium lead (WCLL) blanket was proposed by Aubert [9] using uncertainties code URANIE [10] and ROOT [11]. A design process to find optimal design of ITER Lower Cryostat Thermal Shield was presented [12] by Sequential Quadratic method. Although these methods find the optimal solution under certain conditions, most of them are single-objective optimization and do not optimize the key parameters of the blanket. Yet, these research illustrate that intelligent optimization algorithms are a potential tool that can be applied to the optimization of the blanket.

Therefore, an intelligent optimization method for CFETR HCSB blanket is designed based on a proposed multi-objective NSGA-III algorithm with the adaptive scale factor and the mutation operator of DE algorithm, and an adaptive BP neural network. The proposed method has been validated by the international standard function, then it applied to the optimization design of CFETR HCSB blanket. Based on the proposed method and the Python script, neutronics and thermal input files can be automatically modified and iterated so as to find the optimal radial arrangement within the limits of material temperature and outlet temperature. Finally, the TBR is maximized and the Dose is minimized, and a series of Pareto Front solutions (i.e., optimal solutions) are obtained such that the TBR and shielding performance of the blanket is improved.

The rest of the paper is arranged as follows: The theory of multi-objective optimization algorithm is introduced, and an intelligent optimization method based on an improved multi-objective NSGA-III algorithm with the adaptive scale factor and the mutation operator of DE algorithm are presented and verified in Section 2; Analysis and discussion of the proposed method of the application results to CFETR HCSB blanket are shown in Section 3; Summarization, limitation and future work are presented in Section 4.

2. Methods

2.1. The improvement and validation of NSGA-III algorithm

The multi-objective optimization design of the CFETR HCSB blanket is usually expected to obtain a Pareto Front [13,14]. Currently, the most typical multi-objective optimization algorithms include: NSGA [15], NSGA-II [16], SPEA [17], SPEA2 [18], PESA-II [19], etc., and the state-of-the-art proposed Non-dominated Sorting Genetic Algorithm III (NSGA-III algorithm) in 2013 [20]. Among which, NSGA-II and NSGA-III are the most representative and widely used. A lot of experiments [21–23] have shown that, especially in comparison in 2020 [24], the NSGA-III algorithm has better optimization performance, and although this may vary depending on the different application case, the percentage of NSGA-III that demonstrates better optimization performance will be higher. For optimization of blanket design, the most key thing is to make TBR maximum and Dose minimum by the optimization algorithm, accordingly, the NSGA-III is selected to be applied to the multi-objective optimization design of blanket due to its better optimization performance.

The NSGA-III can solve a high-dimensional goal space very well by utilizing the reference point technique to boost robustness.

The DE algorithm was proposed by Storn in 1997 [25], it has evolved many mutation strategies [26], thereby improving the population diversity and local optimization ability for the conventional NSGA-III algorithm and obtaining the better Pareto Front.

Improvement 1: Introducing the mutation operation of the DE algorithm for the NSGA-III.

The conventional NSGA-III has inherent shortcoming that a narrowly diverse population and poor search ability for solving multi-objective optimization because of the instinctive complex mechanism of genetic algorithm [27]. Rudolph [28] has proved that the conventional GA will never converge to the global optimum only by the three conventional operators. To address this disadvantage, the mutation operation of GA algorithm was replaced by the mutation operation of the DE algorithm to expand the diverse population and search ability of the NSGA-III. Moreover, the mutation strategy that can guarantee the best individuals of the previous generation will definitely be selected for the next generation of crossover operation was adopted. This expression is:

$$\vec{v}_i^G = \vec{x}_{best}^G + F*\left(\vec{x}_{r_1}^G - \vec{x}_{r_2}^G\right), r_1 \neq r_2 \neq best\ ,\ i = 1, 2, \ldots NP \tag{1}$$

Where: $\vec{x}_i^G$ denotes an randomly selected individual from the population $i \in (1, NP)$, G denotes the current generation, $\vec{x}_{best}^G$ denotes one of the best individual in the G th generation, NP denotes the population size, and F denotes the constant scale factor.

Improvement 2: Introducing an adaptive scale factor F.

Furthermore, the conventional NSGA-III algorithm also has disadvantages of some excellent children genes cannot be inherited leading to a significant reduction, in particular, the convergence of the algorithm becomes markedly slower at the later stages of the algorithm due to its use of a constant scale factor. To address this disadvantage, an adaptive scale factor was introduced, thus, the conventional fixed F value:

$$F = F_{constant} \tag{2}$$

Chang to the adaptive F function:

$$F = F_{min} + \Delta F*\cos\left(\frac{\pi}{2}*\frac{G}{G_{max}}\right) \tag{3}$$

Where: F is the scale factor value of the G th generation, F_{min} is the minimum scale factor value, ΔF denotes the variation range of the scale factor, G denotes the current generation, and G_{max} denotes the maximum generation.

This function was chosen as a dynamic adaptive function mainly because:

1) This function satisfies the monotonic decreasing property to ensure the overall decreasing trend of the F, and chooses a larger F value in the prophase of the algorithm, focusing on its global search solution ability, and a smaller F value in the anaphase of the algorithm, focusing on its local search solution ability.

2) This function is a convex function in the definition domain, which is more in line with the overall optimization idea of focusing on the global search solution ability in the prometaphase of optimization, and focusing on the local search solution ability in the anaphase of optimization.

Meanwhile, the values of parameters are also important, and Das [29] found that the algorithm performs better for F ∈ (0.4,0.95) and CR ∈ (0.1,0.8), where CR is preferred to 0.5.

Thus, the improvement strategy of adaptive scale factor and mutation operation of DE algorithm were added to the conventional NSGA-III framework. The pseudo-code of the proposed NSGA-III is as follows.

The 12 international benchmark optimization functions (The DTLZ series functions, The ZDT series functions [30]) were used to validate the correctness and efficiency of the improved NSGA-III algorithm. The four commonly used indicators were chosen as evaluation criteria for the optimization algorithm, namely GD, IGD, HV, and Spacing [31]. The smaller the GD, IGD, and Spacing value, the better the convergence and Spread, and the larger the HV value, the better the uniformity.

Then, the optimization performance of the conventional and improved NSGA-III were compared by the 12 international optimization functions and the four evaluation indicators. The parameter $\boldsymbol{F}$ of the conventional NSGA-III is set to 0.5, the parameters $\boldsymbol{F_{min}}$ and the $\Delta\boldsymbol{F}$ of the improved NSGA-III are set to 0.4 and 0.1. The rest

The Proposed NSGA-III Algorithm in this paper.

Input: H structured reference points Z^s, Initial Population P_0, Population size N, Maximum generation G_{max}, Each individual dimension D, $CR, F_{min}, \Delta F, \vec{x}_{up}$ and $\vec{x}_{low}$

Output: $\boldsymbol{P_{t+1}}$

Initialization: $G = 0, \forall i \le N \cap j \le D: x_{i,j}^{(0)} = x_{i,j,low}^{(0)} + rand(0,1) * \left(x_{i,j,up}^{(0)} - x_{i,j,low}^{(0)}\right)$

while $G < G_{max}$ **do**

while $i \le N$ **do**

1. a children population Q_t is generated by DE algorithm with mutation and crossover from P_t:

(Randomly selection) $r_1, r_2 \in \{1,2,\cdots,N\}$, $r_1 \ne r_2 \ne i$

if $\left(\forall j: rand_j[0,1) < CR \cup j = j_{rand}\right)$ **then**

$$u_{i,j}^G = x_{j,r_{best}}^G + (F_{min} + \Delta F * \cos(\frac{\pi}{2} * \frac{G}{G_{max}})) * (x_{j,r_1}^G + x_{j,r_2}^G)$$

else

$$u_{i,j}^G = x_{i,j}^G$$

end if

2. a combined population $R_t = P_t \cup Q_t$ is generated

3. R_t is divided into a lot of non-domination levels F_1, F_2, F_3,…

4. set $S_t = \emptyset$, $k = 1$,

while size $(S_t) \le N$ **do**

$S_t = S_t \cup F_k$; $k = k + 1$

end

if size $(S_t) = N$ **do**

$P_{t+1} = S_t$; break

else

$P_{t+1} = \cup_{i=1}^{l-1} F_i$

objectives is normalized

reference set Z^r is created according Z^s

each member s of S_t is associate with reference points

a new population is generated by using Niche-Preservation

end

$t = t + 1$

end if

of the settings are the same. The optimization code was performed 50 times for each DTLZ and ZDT functions, and the average calculation results are shown in Table 1 (Bold means win).

By comparing the result, the improved NSGA-III algorithm outperforms the conventional NSGA-III algorithm in most cases. There are 48 comparisons mentioned above, and the improved NSGA-III prevails in 33, two algorithms tied in 11, and the conventional NSGA-III prevails in 4. Therefore, the improved NSGA-III algorithm performs better in terms of the optimization ability, which proves the correctness and efficiency of the improved strategies. Therefore, the proposed algorithm with two improvements described above can significantly improve the optimization performance and was utilized to the blanket design.

2.2. The presentation of an adaptive back propagation (BP) neural network

The functions of BP neural network mainly include regression and classification, etc. The BPNN is utilized to learn certain data mapping relations without prior disclosure of the mathematical equations describing these mapping relations.

An adaptive BP neural network method with learning rate decay and a corresponding a training set sampling based on prior knowledge has been proposed and validated by five radiation field reconstruction cases from our group previous research [32]. The proposed method shows a very excellent predictive performance accompanied by an extremely fast prediction speed.

With the merits of this method, it will be coupled with the NSGA-III algorithm in Section 3, so as to improve the optimization speed.

2.3. The design of the intelligent optimization method based on an improved NSGA-III and an adaptive BP neural network

It is very noteworthy that it is laborious and expensive to only rely on pure NSGA-III optimization algorithm with software simulations to find the global Pareto Front. Because the average time to compute one-time blanket (include neutronics and thermal modeling) model is about 2 min in the optimization process of the post-experiment, and when the population size is set to 30 and the maximum generation is set to 100, it takes roughly 12 days when the optimization algorithm is executed three times.

To address this problem, the use of neural network models instead of software simulation to speed up the optimization process is a viable solution. In the post-experiment, a generation of thirty populations in the optimization algorithm with neural network can be calculated in less than 1 s, which is a 120 times improvement in the efficiency of single model optimization. Especially for full-scale model simulations, which require lower statistical error, the optimization efficiency will be significantly improved by using BP neural network to accelerate the process. Therefore, the application of BP neural network to replace the process of software simulation is a necessary for find the global Pareto Front.

But for the above method, there are inevitable errors of neural network prediction and software simulation calculation. Thus, the real data in current optimization were added to the training set and then the BP neural network was retrained to obtain a neural network with higher accurate prediction at the location of Pareto Front. Then, the NSGA-III algorithm coupled with BP neural network code was executed again and again until the error between the neural network prediction and the software simulation calculation is less than 5%, the update of the neural network model was stopped. Finally, the Pareto Front of blanket optimization was determined according to the value calculated by the software simulation.

Thus, according to the design of the intelligent optimization method based on an improved NSGA-III and an adaptive BP neural network, the efficiency and global solutions of the intelligent optimization of the blanket can be considerably improved.

The flow chart of HCSB blanket optimization based on the intelligent optimization method is shown in Fig. 1.

Table 1
Comparison of the optimization results with 12 international benchmark optimization function.

Name	Type	GD	IGD	HV	Spacing
DTLZ1	conventional NSGA-III	9.29×10^{-6}	1.79×10^{-3}	5.82×10^{-1}	1.55×10^{-4}
	improved NSGA-III	$\mathbf{1.04 \times 10^{-7}}$	$\mathbf{1.78 \times 10^{-3}}$	5.82×10^{-1}	$\mathbf{1.61 \times 10^{-6}}$
DTLZ2	conventional NSGA-III	3.81×10^{-6}	3.96×10^{-3}	3.47×10^{-1}	$\mathbf{6.08 \times 10^{-3}}$
	improved NSGA-III	$\mathbf{3.07 \times 10^{-6}}$	$\mathbf{3.93 \times 10^{-3}}$	$\mathbf{3.48 \times 10^{-1}}$	6.11×10^{-3}
DTLZ3	conventional NSGA-III	4.39×10^{-4}	7.17×10^{-3}	3.41×10^{-1}	7.15×10^{-3}
	improved NSGA-III	$\mathbf{5.28 \times 10^{-6}}$	$\mathbf{3.97 \times 10^{-3}}$	$\mathbf{3.47 \times 10^{-1}}$	$\mathbf{6.23 \times 10^{-3}}$
DTLZ4	conventional NSGA-III	4.08×10^{-7}	3.96×10^{-3}	3.47×10^{-1}	6.02×10^{-3}
	improved NSGA-III	$\mathbf{3.20 \times 10^{-7}}$	3.96×10^{-3}	$\mathbf{3.48 \times 10^{-1}}$	$\mathbf{6.01 \times 10^{-3}}$
DTLZ5	conventional NSGA-III	4.05×10^{-6}	3.96×10^{-3}	3.47×10^{-1}	6.07×10^{-3}
	improved NSGA-III	$\mathbf{3.33 \times 10^{-6}}$	3.96×10^{-3}	3.47×10^{-1}	$\mathbf{6.03 \times 10^{-3}}$
DTLZ6	conventional NSGA-III	3.66×10^{-6}	3.96×10^{-3}	3.47×10^{-1}	6.09×10^{-3}
	improved NSGA-III	$\mathbf{3.09 \times 10^{-6}}$	$\mathbf{3.95 \times 10^{-3}}$	$\mathbf{3.50 \times 10^{-1}}$	$\mathbf{6.07 \times 10^{-3}}$
DTLZ7	conventional NSGA-III	3.38×10^{-5}	5.03×10^{-3}	2.42×10^{-1}	1.63×10^{-3}
	improved NSGA-III	$\mathbf{6.46 \times 10^{-6}}$	$\mathbf{4.82 \times 10^{-3}}$	2.42×10^{-1}	$\mathbf{9.88 \times 10^{-4}}$
ZDT1	conventional NSGA-III	4.02×10^{-6}	3.88×10^{-3}	7.20×10^{-1}	1.00×10^{-2}
	improved NSGA-III	$\mathbf{3.75 \times 10^{-6}}$	3.88×10^{-3}	7.20×10^{-1}	1.00×10^{-2}
ZDT2	conventional NSGA-III	4.22×10^{-6}	3.80×10^{-3}	4.45×10^{-1}	4.10×10^{-3}
	improved NSGA-III	$\mathbf{7.66 \times 10^{-7}}$	$\mathbf{3.79 \times 10^{-3}}$	4.45×10^{-1}	$\mathbf{3.18 \times 10^{-3}}$
ZDT3	conventional NSGA-III	3.13×10^{-5}	5.90×10^{-3}	5.82×10^{-1}	1.15×10^{-2}
	improved NSGA-III	$\mathbf{2.86 \times 10^{-5}}$	$\mathbf{5.55 \times 10^{-3}}$	$\mathbf{5.83 \times 10^{-1}}$	$\mathbf{1.05 \times 10^{-2}}$
ZDT4	conventional NSGA-III	$\mathbf{2.00 \times 10^{-5}}$	$\mathbf{3.90 \times 10^{-3}}$	7.20×10^{-1}	$\mathbf{9.89 \times 10^{-3}}$
	improved NSGA-III	1.95×10^{-4}	2.26×10^{-2}	$\mathbf{9.70 \times 10^{-1}}$	3.06×10^{-2}
ZDT6	conventional NSGA-III	3.46×10^{-6}	3.00×10^{-3}	3.88×10^{-1}	1.96×10^{-3}
	improved NSGA-III	$\mathbf{3.11 \times 10^{-6}}$	3.00×10^{-3}	3.88×10^{-1}	$\mathbf{1.93 \times 10^{-3}}$

3. The application of an intelligent optimization method for HCSB blanket

3.1. The introduction of the CFETR HCSB blanket

CFETR is a proposed tokamak fusion reactor [33], the HCSB blanket was proposed as one of the main candidate blanket for CFETR, the 3D simplified CFETR model and blanket module as shown in Fig. 2 (a) and (b), respectively, the blanket module is mainly composed of the first wall (FW), breeding zones (Be and Li4SiO4), cooling plates (CPs), backplate and attachment systems [34]. The blanket module No.12 in Fig. 2(a) was chosen to the research object due to it experiences the most serious neutron irradiation and suffers the maximum neutron wall loading [35].

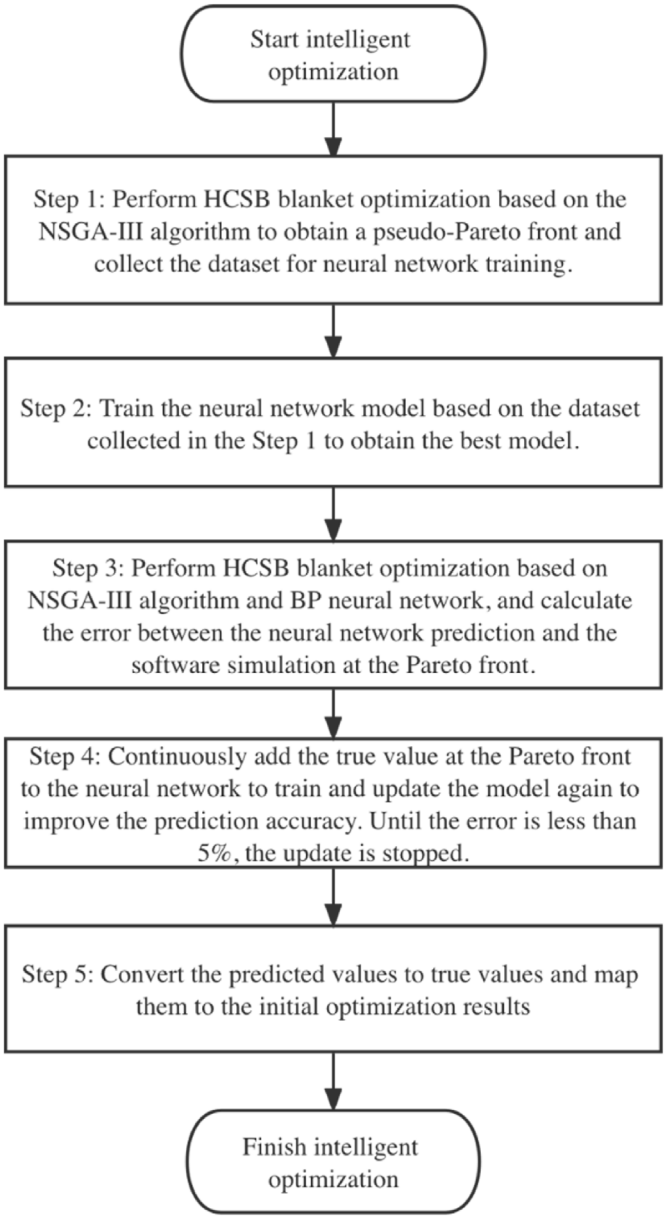

Fig. 1. The flow chart of HCSB blanket optimization based on the intelligent optimization method.

3.2. Design and implementation of the optimized model

3.2.1. The selection of optimization variables and optimization objectives

Considering that one of the critical factors for the 3D blanket design is the radial arrangement of the functional zone [36], radial arrangement was firstly selected as the optimization variable. The key parameters of the blanket: the TBR and the Dose are used as optimization objectives.

3.2.2. The simplification and setup of simulation model

If the full-scale 3D model is used for calculation analysis, it will become very time-consuming, and make the optimization process extremely redundant. Therefore, the 3D neutronics and 2D planar thermal-hydraulic simulation models, which share the same geometry, material, and properties, are simplified as shown in Fig. 2 (c) and (d).

SuperMC software [37] and the IAEA Fusion Evaluation Nuclear Database FENDL-3.0 [38] are used as neutronics simulation. Fluent 14.0 [39] and Ansys Parameter Design Language 14 (APDL 14) are used as thermal-hydraulics simulation.

The geometry and computational setting of the CFETR HCSB blanket are listed in Tables 2 and 3, more detailed material information and boundary conditions are available in these literatures [40–42].

3.2.3. The implementation of CFETR HCSB blanket optimization design

For the optimization of blanket design, it is difficult to satisfy all the optimization variables and optimization objectives in engineering practice. Therefore, in this paper, only the following optimization variables, optimization objectives and constraints condition are selected, without considering all possible optimization criteria.

Optimization variables: the radial length of the functional zones, that is, four Be breeding zones (X1, X3, X5, X7) and three Li_4SiO_4 breeding zones (X2, X4, X6), as shown in Fig. 3. The seven breeding zones were determined based on the previous studies and experience, and the number of Li_4SiO_4 and Be will also be optimized in the future research.

Optimization objectives:

1) Making the TBR of the whole HCSB blanket as larger as possible.
2) Making the Dose of the backplane of the HCSB blanket as lower as possible.

Constraint condition:

1) The temperature of all components of the whole HCSB blanket not exceed the limit.
2) The radial length of functional zone remains unchanged, that is, Σ Xi = 553 mm.
3) The outlet temperature is about 500 °C (to avoid creep strength drop temperature).

These are an inevitable constraint condition for the blanket optimization design, so the penalty function is introduced into the improved NSGA-III [43]. In terms of constraint condition, the main considerations are whether the outlet temperature and material temperature of the design solution exceed the limits and whether the radial functional length meets the design requirements. The strategy for handling the constraint condition is based on the following two principles:

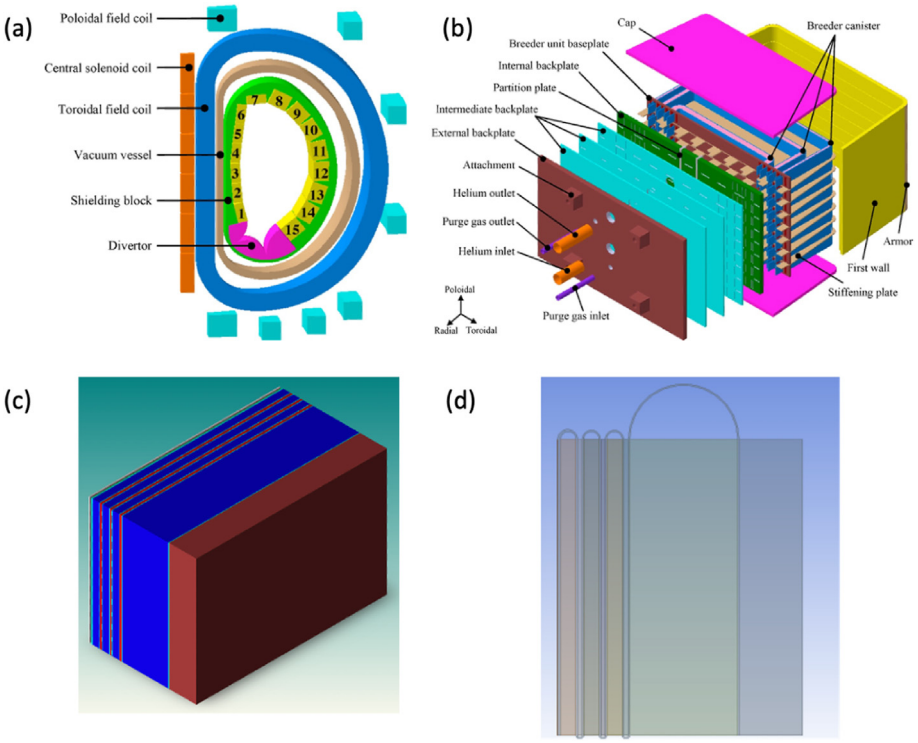

Fig. 2. The CFETR HCSB blanket and simplified simulation model.

Table 2
Main materials of the No. 12 blanket.

Item	Materials and Temperature limitation
structure material	Reduced Activation Ferritic/Martensitic (RAFM), The temperature of RAFM and these pipes does not exceed 550 °C.
First wall	Tungsten, the temperature of W armor does not exceed 1300 °C.
tritium breeder	Lithium ceramic of Li_4SiO_4 pebble with 90% 6Li enrichment with packing factor about 62%, 400 °C < The temperature of Li4SiO4 < 920 °C
neutron multiplier	Beryllium pebble bed with packing factor about 80%, 300 °C < The temperature of Be < 650 °C

Table 3
Neutronics and thermal hydraulics computational boundary setup of the No. 12 blanket.

Item	Value or Setting
parametric plasma neutron source/MeV	14
coolant	8 MPa helium gas
coolant inlet/outlet temperature/°C	300/500
Wall roughness/mm	0.2
Turbulence model	k–ε
Top, bottom, left, and right surfaces of neutronics model	Reflection boundary
Back surface of neutronics model	Transmitting boundary
Top, bottom and back surfaces of thermal-hydraulic model	Adiabatic boundary
Top and bottom surfaces of the connecting elbow pipes	Adiabatic, no slip wall
The convergence criterion of the neutronics calculation	Less than 2% relative statistical error
The convergence criterion of the thermal-hydraulic calculation	The default convergence residual errors are less than 1×10^{-2} for velocity, turbulent kinetic energy and turbulent kinetic energy dissipation, and less than 1×10^{-8} for pressure and temperature.

1) When both parents and children violate the constraint or not, the individual that violates the lesser constraint is selected.
2) When only one of the parents and children violates the constraint, the individual that does not violate the constraint is selected.

One thing to point out here is that the "TBR" of simplified 3D neutronics model is generally larger than accurate 3D neutronics model [44], thus, the TBR in this paper is only employed to measure the trend of change; moreover, the design constraints such as fuel consumption and structural stress are not considered in this paper, and only the temperature and radial length are used to satisfy the constraints. This paper mainly focuses on the study of intelligent optimization method for blanket, and only need to add additional

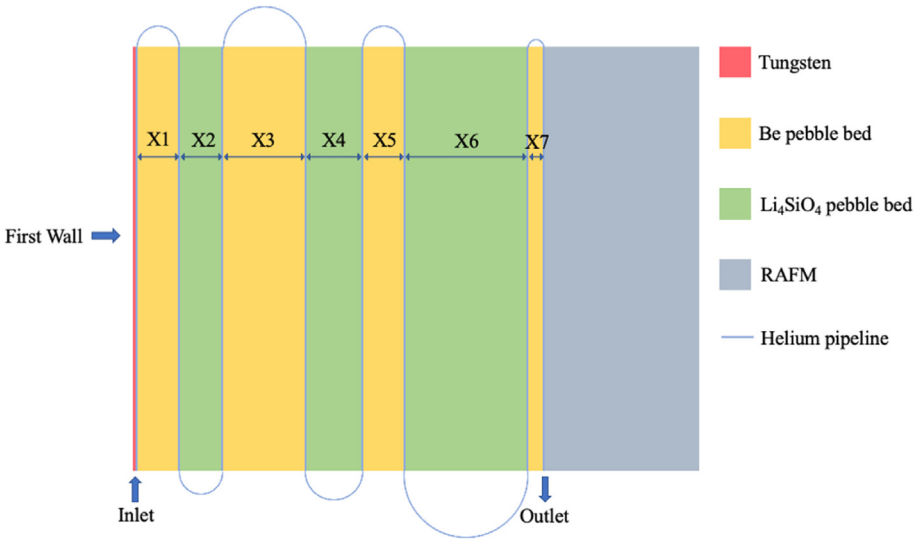

Fig. 3. The simplified blanket simulation model for optimization design.

these constraints when fuel consumption and structural stress need to be considered, which does not affect the correctness and efficiency of the optimization methods.

The PyCharm with Python3.8 is used as a development platform for the optimization design of blanket model.

The main application process of the improved NSGA-III algorithm in the CFETR HCSB blanket is provided as follows and the flow chart is given in Fig. 4:

Step1: The initial parameters of the radial length of the functional zone of the HCSB blanket was randomly generated and coding by the improved NSGA-III algorithm;
Step2: The neutronics geometric model and thermal-hydraulic geometric model was generated by decoding parameters generated in Step1, all neutronics and thermal-hydraulic computational boundary settings (e.g., neutron source distribution, geometric structure of each cell and plane, properties and density of each material, etc.) are set according to design requirements;
Step3: The TBR, Dose, and the Nuclear Power Deposit (NPD) were calculated by calling the SuperMC software for neutron transport calculations;
Step4: Through the proposed data mapping script based on Python, the NPD was transferred to thermal-hydraulic model calculations as an internal heat source, then building the thermal-hydraulic model of the blanket and generating the mesh, the outlet temperatures and the temperatures of the components in the functional zone were calculated by calling the Fluent software;
Step5: Based on the improved hybrid NSGA-III and DE algorithm ideas of parent's mutation and crossover, the children were generated, repeat Step2, Step3, Step4, the parent's and children's blanket design cases were evaluated by penalty function, and selected the more excellent design cases in both generations to retain.
Step6: Repeated Step5 until the specified number of evolutionary generations was completed, then a Pareto Front solution was obtained.

The setup of improved NSGA-III algorithm is shown in Table 4.

3.3. Optimization results

The process of Fig. 1 was implemented in this section 3.3. The improved NSGA-III algorithm was first applied to the optimization design of the CFETR HCSB blanket based on the Step1 in Fig. 1. The optimization algorithm was executed three times that take roughly 12 days, and then the three optimizations results were combined after manually deleting some solutions outside the constraint, as shown in Fig. 5 and Table 5. Each point in Fig. 5 is a feasible solution generated by the optimization algorithm, the red dots indicate the optimal solution. Fig. 5 shows that the improved NSGA-III algorithm is effective in optimizing the HCSB blanket, which locates the Pareto Front, that is, maximizing the TBR and minimizing the dose.

As described in section 2.3, strictly speaking, the current optimization result is not guaranteed to be the global optimal solution, and therefore, the validity of the Pareto Front of Fig. 5 is open to question since it is too time consuming to only rely on software simulation calculation.

Consequently, an adaptive BP neural network with a training set sampling based on prior knowledge based improved NSGA-III optimization algorithms will be applied to the optimal design of the HCSB blanket. This neural network was employed to replace the software simulation calculations of SuperMC and Fluent 14.0, so as to accelerate the optimization process. In terms of finding the globally optimal Pareto Front, the aim of Fig. 5 is to find a pseudo-Pareto Front (as a reference and benchmark for the global optimal Pareto Front) and to collect the training set for future neural network training.

Based on the adaptive BP neural network principle of a training set sampling:

1) To sample as randomly and uniformly as possible in objective space, Latin hypercube sampling [45] was first performed in the domain of the optimization variables, and a total of 4800 Latin hypercube sampling points are created.
2) Then based on the empirical knowledge, 1500 points closest to the Pareto Front in Fig. 5 were also added to the training set due to the highest prediction performance of the neural network is required at the Pareto Front other than at the center of the objective space.

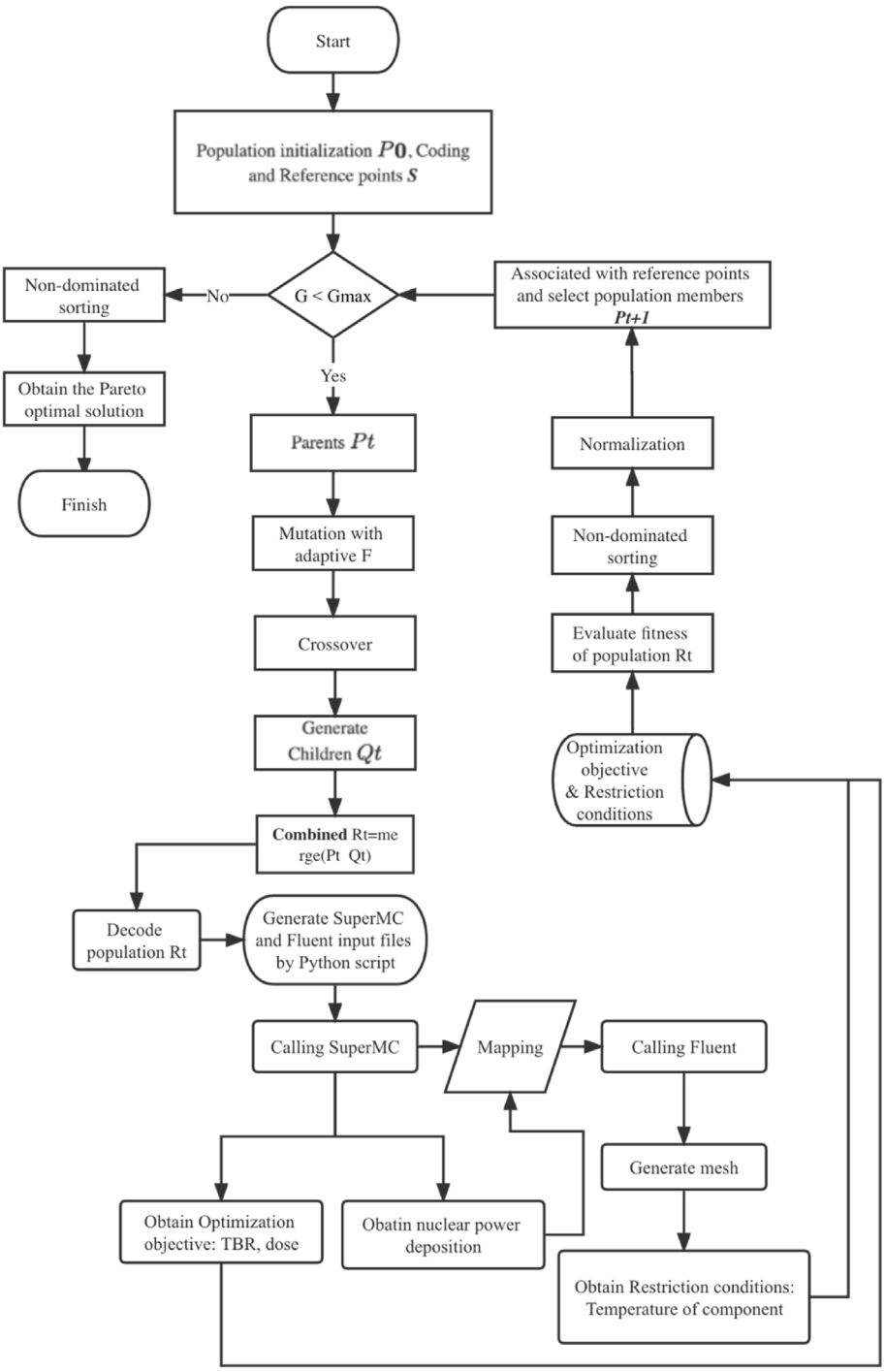

Fig. 4. The flow chart of the application of improved NSGA-III algorithm for CFETR HCSB blanket.

Table 4
The setup of improved NSGA-III algorithm.

Item	Value
Population size	30
Maximum generations	100
Initial differential scale F	0.4
CR	0.7
Domain of optimization variables	Be∈[0.05 m, 0.2 m] Li∈[0.02 m, 0.09 m]

Therefore, there are 6300 data sets for the neural network, of which 6000 are randomly selected as the training set and the remaining 300 are used as the test set.

The optimization variables is used as the input of the neural network, the TBR, Dose, outlet temperature, and maximum temperature of each component of this blanket are used as the output. The neural network was trained and implemented under the TensorFlow framework using the Python environment. The search steps of the neural network topology are as follows: the search space is extended to 1–3 layers with a maximum of 150 nodes, and

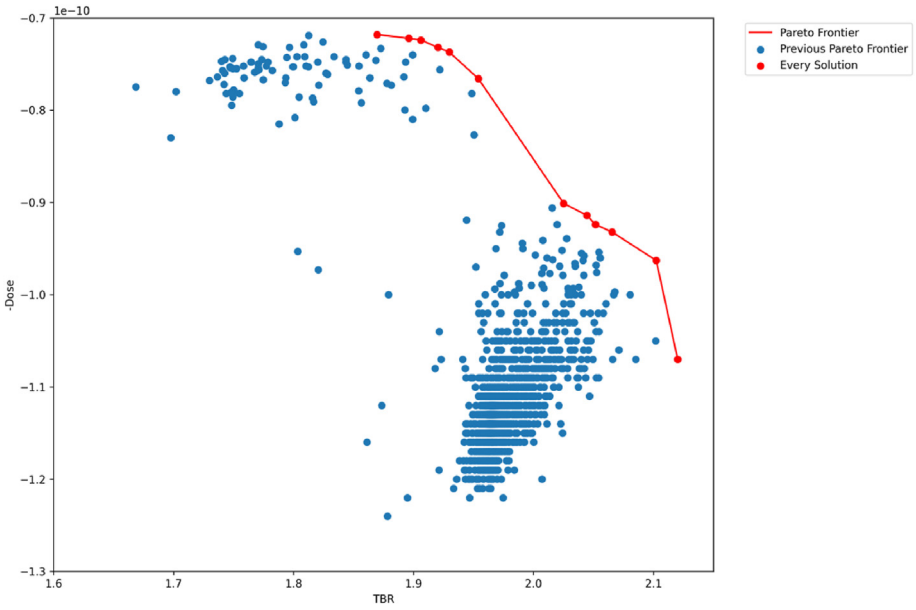

Fig. 5. The Pareto optimal solutions of CFETR HCSB blanket by improved NSGA-III algorithm.

Table 5
Results of blanket optimization by improved NSGA-III algorithm.

No.	x1 (unit: m)	x2	x3	x4	x5	x6	x7	TBR	Dose (unit: rem/hr)
1	0.08894	0.03885	0.11741	0.06129	0.15112	0.08882	0.00656	1.870	7.18E-11
2	0.07191	0.03934	0.10723	0.04208	0.20000	0.09000	0.00244	1.896	7.22E-11
3	0.07310	0.03613	0.10723	0.04261	0.20000	0.09000	0.00394	1.906	7.24E-11
4	0.07100	0.02987	0.10543	0.04475	0.20000	0.08989	0.01207	1.920	7.32E-11
5	0.05000	0.02200	0.10664	0.05500	0.20000	0.07676	0.04260	1.930	7.37E-11
6	0.07310	0.02000	0.09677	0.03084	0.19055	0.08137	0.06038	1.954	7.66E-11
7	0.07781	0.02000	0.08850	0.03834	0.19999	0.07574	0.05262	2.025	9.01E-11
8	0.06983	0.02344	0.09720	0.04124	0.20000	0.08989	0.03140	2.045	9.14E-11
9	0.07782	0.02554	0.12844	0.04263	0.16278	0.09000	0.02579	2.052	9.24E-11
10	0.07252	0.02000	0.09516	0.02000	0.19825	0.07130	0.07577	2.065	9.32E-11
11	0.05687	0.02900	0.11931	0.02996	0.20000	0.06826	0.04961	2.102	9.63E-11
12	0.05285	0.04558	0.12100	0.02411	0.20000	0.06286	0.04661	2.120	1.07E-10

the topology was selected at this time when the loss function value is minimum and tend to converge. By the above operation, the parameter settings and prediction results of the adaptive BP neural network model are shown in Table 6.

Then the ten neural network models in Table 6 were used directly to predict the TBR, Dose, outlet temperature, and temperature of each component of the blanket model, and they were used as the optimization objectives and constraints condition of the improved NSGA-II algorithm.

Table 6
Parameter settings and prediction results of the adaptive BP neural network model.

Algorithm settings	TBR	Dose	t	Be1	Li1
Layer number	3	3	2	2	2
Batch Size	256	256	384	256	384
Nodes number per layer	100,80,60	128,64,16	128,64	256,64	256,64
Activation function	Softsign	Tanh	Softsign	Softsign	Softsign
Test set MRE	5.64%	2.37%	0.31%	0.33%	8.91%
Algorithm settings	**Be2**	**Li2**	**Be3**	**Li3**	**Be4**
Layer number	2	2	2	2	2
Batch Size	384	384	384	384	384
Nodes number per layer	128,64	256,128	64,64	64,64	32,64
Activation function	Softsign	Softsign	Softsign	Softsign	Softsign
Test set MRE	1.43%	1.92%	0.79%	2.44%	0.63%

The optimization flow chart for HCSB blanket based on adaptive BP neural network and improved NSGA-III optimization algorithm is shown in Fig. 6. The flow is almost the same as Fig. 4, but the previous values obtained by software simulation were predicted by the neural network model. For the calculation speed, the optimization that originally take twelve days can be done within 5 min now.

The three optimizations were executed again according to Fig. 6, and then the three optimizations results are combined after manually deleting some solutions outside the constraint, as shown in Fig. 7 and Table 7. It shows that the optimization algorithm based on the adaptive BP neural network prediction still finds the Pareto Front, maximizes the TBR and minimizes the Dose.

According to the comparison of the two Pareto Fronts in Fig. 7 and Table 7 (where Pre_ in Table 7 represents the value obtained based on the neural network prediction and Real_ is the value obtained from the software simulation calculation), there is a gap between the two Pareto Fronts, and their average relative errors of TBR and Dose are 4.34% and 9.21%, respectively. It's worth noting that the NSGA-III algorithm based on neural network is faster than the pure NSGA-III algorithm, so more populations can be set up to find the optimal solution (50 populations are set in Fig. 7), and this is an advantage of finding a better solution in terms of the absolute

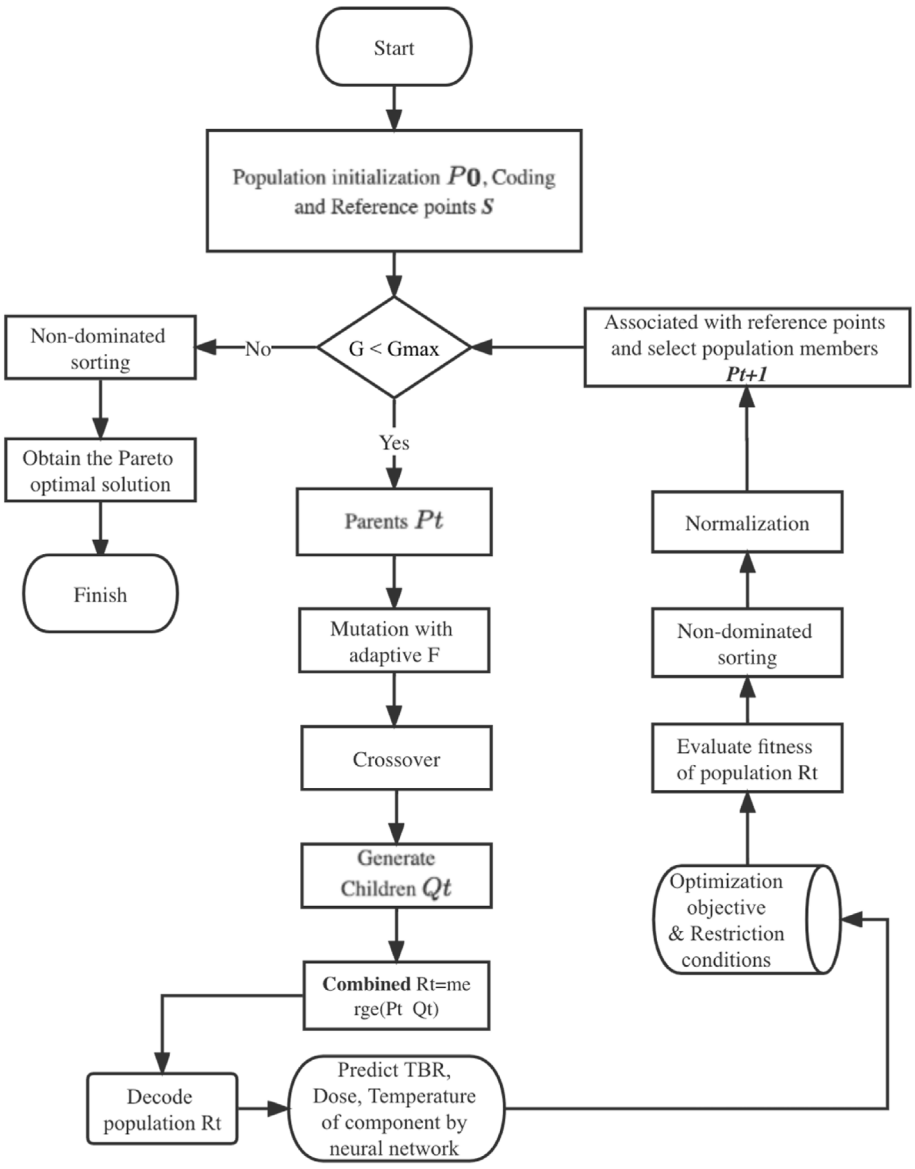

Fig. 6. The flow chart of the application of improved NSGA-III algorithm and adaptive BP neural network for CFETR HCSB blanket.

number of populations.

To further find the better and real Pareto Front according to the flow in Fig. 1, the real data in Table 7 were added to the training set and the neural network was retrained until the error between the neural network prediction and the software simulation calculation is less than 5%. After two iterations of the neural network, the MRE of the TBR and Dose obtained by the neural network calculation and simulation software are 3.39% and 4.87%, respectively, as shown in Table 8 and Fig. 8. If a lower MRE is desired, using a neural network model with an acceptable prediction time and a prediction MRE below 10^{-5} is a potential solution.

From a mathematical point of view, the final Pareto Front of the blanket optimization (eleven solutions in total, as shown in Fig. 9, and Table 9) was found by the proposed an intelligent optimization method, which is also better than the Pareto Front in Fig. 5 of pure NSGA-III algorithm only calculated by software simulation.

From a neutronic and dose point of view, the maximized TBR are between 1.87 and 2.12, which all meet the requirements of maintaining tritium self-sustainability; the minimized Dose are also at an acceptable level according to the recommended dose rate for the reactor shutdowns [46], which meets the advanced remote operation requirements in the United States. Since this paper considers the Dose of the whole backplane and the physical model of simulation is a solid entity, it is higher than the reality of the backplane dose rate with many pipes and pipe holes.

Therefore, it is proved that the proposed intelligent optimization method for blanket optimization has significant optimization effect, and the efficiency of CFETR HCSB blanket optimization design is remarkably improved, the optimal design of the blanket is achieved under certain constraints.

4. Conclusion and future work

This paper proposes an intelligent optimization method for CFETR HCSB blanket based on an improved multi-objective NSGA-III algorithm and an adaptive BP neural network. The innovations and contributions of this paper are as follows:

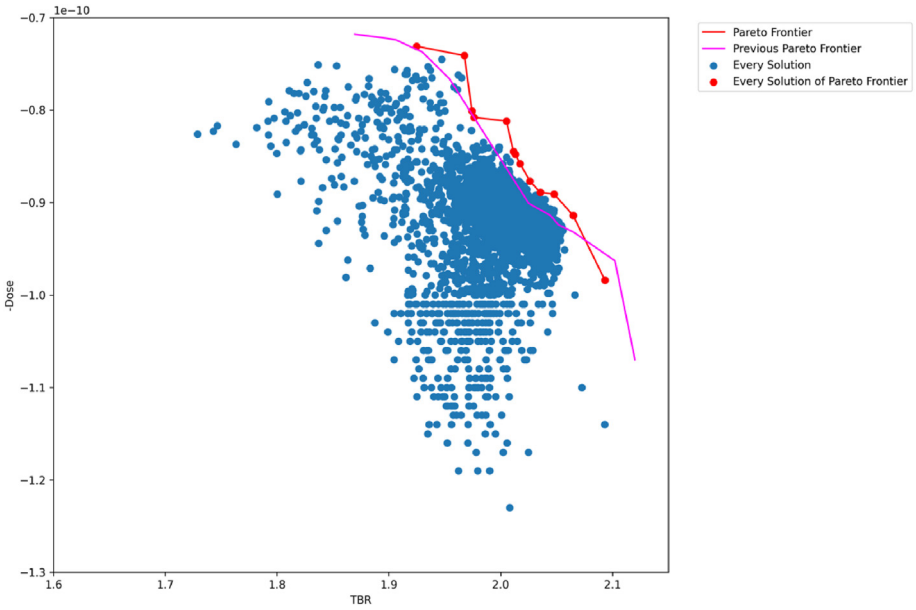

Fig. 7. The Pareto optimal solutions of CFETR HCSB blanket based on improved NSGA-III algorithm and adaptive BP neural network.

Table 7
Results of blanket optimization based on improved NSGA-III algorithm with adaptive BP neural network.

No.	x1	x2	x3	x4	x5	x6	x7
1	0.05828	0.03762	0.14283	0.03647	0.19217	0.06732	0.01832
2	0.07340	0.03021	0.11308	0.06101	0.16718	0.09000	0.01812
3	0.05211	0.02161	0.10369	0.03554	0.20000	0.08002	0.06003
4	0.05000	0.02000	0.11304	0.04425	0.17667	0.09000	0.05904
5	0.05211	0.02104	0.10060	0.04429	0.19119	0.08975	0.05403
6	0.06664	0.02717	0.10561	0.03367	0.19660	0.08505	0.03826
7	0.05156	0.03253	0.15231	0.02000	0.15073	0.08618	0.05969
8	0.05000	0.02418	0.10956	0.02000	0.18779	0.08143	0.08004
9	0.07532	0.02000	0.20000	0.07826	0.05000	0.09000	0.03942
10	0.06809	0.02243	0.20000	0.04798	0.11347	0.09000	0.01103
11	0.06465	0.03615	0.14739	0.03000	0.20000	0.06841	0.00641
12	0.06581	0.02025	0.09473	0.02000	0.19959	0.08513	0.06749
13	0.05159	0.03163	0.11853	0.02386	0.20000	0.09000	0.03739

No.	Pre_TBR	Pre_Dose	Real_TBR	Real_Dose	TBR_MRE	Dose_MRE
1	1.974	8.01E-11	1.871	7.42E-11	0.055	0.080
2	1.976	8.08E-11	1.811	7.22E-11	0.091	0.119
3	2.017	8.58E-11	1.886	7.67E-11	0.070	0.119
4	2.011	8.45E-11	1.951	7.49E-11	0.031	0.127
5	2.026	8.77E-11	1.868	7.57E-11	0.085	0.158
6	2.048	8.91E-11	2.073	9.42E-11	0.012	0.054
7	2.013	8.48E-11	2.133	9.96E-11	0.056	0.149
8	2.035	8.89E-11	1.973	7.69E-11	0.032	0.157
9	1.925	7.31E-11	1.834	7.51E-11	0.049	0.026
10	1.968	7.41E-11	1.986	7.35E-11	0.009	0.008
11	2.005	8.12E-11	2.122	9.92E-11	0.055	0.181
12	2.065	9.14E-11	2.079	9.20E-11	0.007	0.006
13	2.093	9.84E-11	2.121	9.72E-11	0.013	0.013

Table 8
Results of blanket optimization based on improved NSGA-III algorithm and two iterations of the adaptive BP neural network.

No.	x1	x2	x3	x4	x5	x6	x7
1	0.060	0.021	0.124	0.044	0.176	0.080	0.044
2	0.075	0.025	0.177	0.029	0.187	0.049	0.010
3	0.068	0.020	0.187	0.052	0.122	0.089	0.014
4	0.072	0.020	0.184	0.060	0.116	0.075	0.026
5	0.073	0.037	0.123	0.020	0.198	0.090	0.011
6	0.050	0.020	0.130	0.051	0.180	0.090	0.031
7	0.078	0.020	0.104	0.053	0.199	0.089	0.009
8	0.053	0.022	0.126	0.028	0.200	0.087	0.036
9	0.066	0.020	0.124	0.029	0.193	0.088	0.033

No.	Pre_TBR	Pre_Dose	Real_TBR	Real_Dose	TBR_MRE	Dose_MRE
1	1.987	7.960E-11	2.068	8.957E-11	0.039	0.111
2	1.971	7.600E-11	1.893	7.508E-11	0.041	0.012
3	1.969	7.430E-11	1.885	7.373E-11	0.044	0.008
4	1.948	7.430E-11	1.974	7.325E-11	0.013	0.014
5	2.100	9.920E-11	2.111	9.892E-11	0.005	0.003
6	2.013	8.190E-11	1.964	7.444E-11	0.025	0.100
7	2.023	8.310E-11	1.817	7.375E-11	0.113	0.127
8	2.078	8.930E-11	2.115	9.171E-11	0.018	0.026
9	2.070	8.640E-11	2.085	8.967E-11	0.007	0.037

1) The first key issue is to improve the method's optimization performance for the blanket optimization design. Based on the drawbacks existing in the conventional NSGA-III, the strategy of adaptive scale factor and mutation operator is introduced to improve the global and local optimization and population diversity. Then, the improved NSGA-III algorithm is validated by 12 international benchmark optimization functions, and the results indicate the improved NSGA-III has significant optimization performance than the conventional NSGA-III, which proves the correctness and efficiency of the improved strategy.
2) Another key issue is to improve the method's speed for finding Pareto Front for the blanket optimization design. So, an intelligent optimization method based on an improved multi-objective NSGA-III algorithm and an adaptive BP neural network is developed. The adaptive BP neural network-based NSGA-III algorithm is 120 times more efficient than the software computation-based NSGA-III algorithm for a generation of 30 populations. Therefore, more populations can be set up to find the optimal solution, and this is an advantage of finding a better solution in terms of the absolute number of populations.
3) The proposed intelligent optimization method are applied to the HCSB blanket optimization, and the results indicate the optimal design of the HCSB blanket, namely maximizing the TBR and minimizing the Dose, is achieved under certain constraints. This study can provide valuable guidance and reference for the

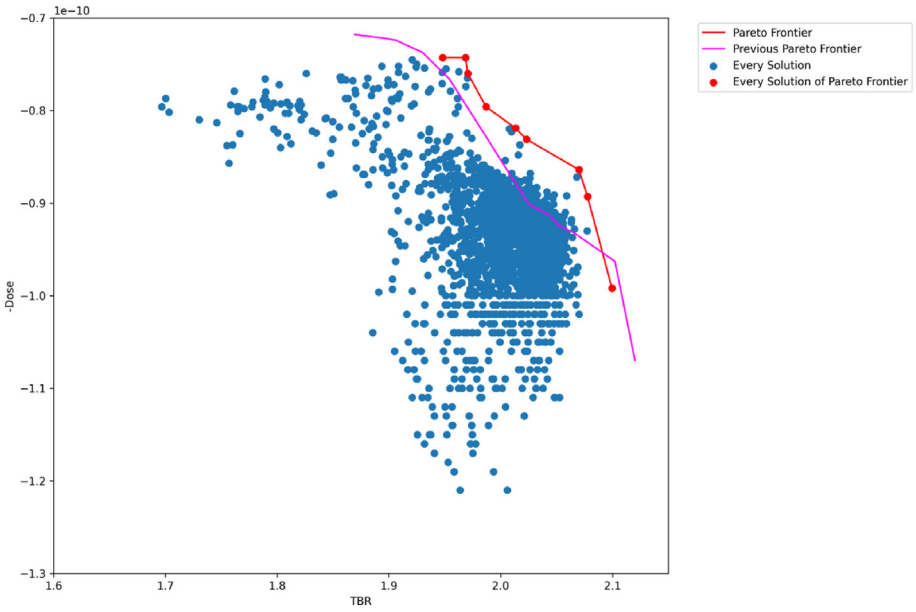

Fig. 8. The Pareto optimal solutions of CFETR HCSB blanket based on improved NSGA-III algorithm and two iterations of the adaptive BP neural network.

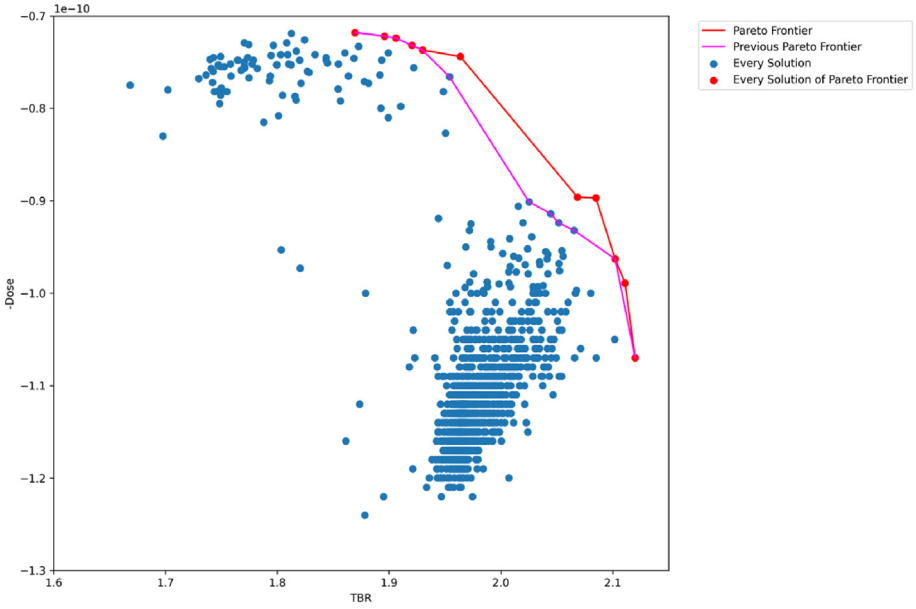

Fig. 9. The final Pareto optimal solutions of CFETR HCSB blanket based on the proposed intelligent optimization method.

Table 9
Final results of blanket optimization based on the proposed intelligent optimization method.

No.	x1	x2	x3	x4	x5	x6	x7	TBR	Dose
1	0.08894	0.03885	0.11741	0.06129	0.15112	0.08882	0.00656	1.870	7.18E-11
2	0.07191	0.03934	0.10723	0.04208	0.20000	0.09000	0.00244	1.896	7.22E-11
3	0.07310	0.03613	0.10723	0.04261	0.20000	0.09000	0.00394	1.906	7.24E-11
4	0.07100	0.02987	0.10543	0.04475	0.20000	0.08989	0.01207	1.920	7.32E-11
5	0.05000	0.02200	0.10664	0.05500	0.20000	0.07676	0.04260	1.930	7.37E-11
6	0.05000	0.02000	0.12986	0.05107	0.17976	0.09000	0.03232	1.964	7.44E-11
7	0.06069	0.02101	0.12447	0.04496	0.17677	0.08030	0.04481	2.068	8.96E-11
8	0.06559	0.02000	0.12353	0.02931	0.19256	0.08780	0.03422	2.085	8.97E-11
9	0.05687	0.02900	0.11931	0.02996	0.20000	0.06826	0.04961	2.102	9.63E-11
10	0.07259	0.03695	0.12348	0.02000	0.19824	0.09000	0.01175	2.111	9.89E-11
11	0.05285	0.04558	0.12100	0.02411	0.20000	0.06286	0.04661	2.120	1.07E-10

conceptual design and comprehensive analysis of the CFETR HCSB blanket.

The proposed method improves the optimization design efficiency of the blanket model to a certain extent. However, there are some limitations in the application of the method, such the optimization design of the blanket currently considers only the functional radial arrangement.

Hence, it is necessary to further perfect the research. In the future, the material selection of blanket, and the number of Li_4SiO_4 and Be, the enrichment of Li-6 can be optimized as hybrid discrete and continuous variables, so as to make the optimization closer to the real world.

Funding

This work was funded by the National Key Research and Development Program of China (2019YFE0191700) and by the Natural Science Foundation of Anhui Province (2008085MA23).

Contributions statement

Wen Zhou: Conceptualization, Formal analysis, Methodology, Writing - original draft, Writing - review & editing. Guomin Sun: Funding acquisition, Validation, Investigation, Supervision, Project administration. Zhuang Li: Investigation, Resources. Di Zhang: Investigation, Resources. Zihui Yang: Funding acquisition, Project administration. Jianye Wang: Project administration, Funding acquisition. Shuichiro Miwa: Investigation, Resources.

Declaration of competing interest

The authors declare that they have no known competing financial interests or personal relationships that could have appeared to influence the work reported in this paper.

References

[1] Y.C. Wu, S. Şahin, Fusion energy production, Compr. Energy Syst. 13 (2018) 538–589, https://doi.org/10.1016/b978-0-12-809597-3.00330-8.
[2] L.M. Giancarli, X. Bravo, S. Cho, et al., Overview of recent ITER TBM Program activities, Fusion Eng. Des. 158 (2020), 111674, https://doi.org/10.1016/j.fusengdes.2020.111674.
[3] X.H. Wu, H.B. Liao, X.Y. Wang, et al., Design optimization and analysis of CN HCCB TBM-set, Fusion Eng. Des. 136 (2018) 839–846, https://doi.org/10.1016/j.fusengdes.2018.04.018.
[4] F. Hernández, P. Pereslavtsev, Q. Kang, et al., A new HCPB breeding blanket for the EU DEMO: evolution, rationale and preliminary performances, Fusion Eng. Des. 124 (2017) 882–886, https://doi.org/10.1016/j.fusengdes.2017.02.008.
[5] F.A. Hernández, F. Arbeiter, L.V. Boccaccini, et al., Overview of the HCPB research activities in EUROfusion, IEEE Trans. Plasma Sci. 46 (2018) 2247–2261, https://doi.org/10.1109/tps.2018.2830813.
[6] F.A. Hernández, P. Pereslavtsev, G. Zhou, et al., Consolidated design of the HCPB breeding blanket for the pre-conceptual design phase of the EU DEMO and harmonization with the ITER HCPB TBM program, Fusion Eng. Des. 157 (2020), 111614, https://doi.org/10.1016/j.fusengdes.2020.111614.
[7] P. Pereslavtsev, U. Fischer, F. Hernandez, et al., Neutronic analyses for the optimization of the advanced HCPB breeder blanket design for DEMO, Fusion Eng. Des. 124 (2017) 910–914, https://doi.org/10.1016/j.fusengdes.2017.01.028.
[8] D. Zhang, S. Cui, J. Cheng, et al., Improving the optimization algorithm of NTCOC for application in the HCSB blanket for CFETR Phase II, Fusion Eng. Des. 135 (2018) 216–227, https://doi.org/10.1016/j.fusengdes.2018.07.027.
[9] J. Aubert, G. Aiello, C. Bachmann, et al., Optimization of the first wall for the DEMO water cooled lithium lead blanket, Fusion Eng. Des. 98 (2015) 1206–1210, https://doi.org/10.1016/j.fusengdes.2015.01.008.
[10] F. Gaudier, URANIE: the CEA/DEN uncertainty and sensitivity platform, Procedia Soc. Behav Sci. 2 (2010) 7660–7661, https://doi.org/10.1016/j.sbspro.2010.05.166.
[11] I. Antcheva, M. Ballintijn, B. Bellenot, et al., ROOT—a C++ framework for petabyte data storage, statistical analysis and visualization, Comput. Phys. Commun. 182 (2011) 1384–1385, https://doi.org/10.1016/j.cpc.2011.02.008.
[12] C.H. Noh, W. Chung, J. Lim, et al., Optimization of the outer support in the ITER lower cryostat thermal shield, Fusion Eng. Des. 103 (2016) 85–92, https://doi.org/10.1016/j.fusengdes.2015.12.014.
[13] C. Coello, C.A. Coello, A short tutorial on evolutionary multiobjective optimization, in: International Conference on Evolutionary Multi-Criterion Optimization, Springer, Berlin, Heidelberg, 2001, pp. 21–40, https://doi.org/10.1007/3-540-44719-9_2.
[14] P. Seferlis, M.C. Georgiadis (Eds.), The Integration of Process Design and Control, Elsevier, 2004, https://doi.org/10.1016/s1570-7946(04)80052-x.
[15] N. Srinivas, K. Deb, Muiltiobjective optimization using nondominated sorting in genetic algorithms, Evol. Comput. 2 (1994) 221–248, https://doi.org/10.1162/evco.1994.2.3.221.
[16] K. Deb, S. Agrawal, A. Pratap, et al., A fast elitist non-dominated sorting genetic algorithm for multi-objective optimization: NSGA-II, in: International Conference on Parallel Problem Solving from Nature, Springer, Berlin, Heidelberg, 2000, pp. 849–858, https://doi.org/10.1007/3-540-45356-3_83.
[17] E. Zitzler, Evolutionary Algorithms for Multiobjective Optimization: Methods and Applications, vol. 63, Shaker, Ithaca, 1999.
[18] E. Zitzler, M. Laumanns, L. Thiele, SPEA2: improving the strength Pareto evolutionary algorithm, TIK-report. 103 (2001), https://doi.org/10.3929/ethz-a-004284029.
[19] D.W. Corne, N.R. Jerram, J.D. Knowles, et al., PESA-II: region-based selection in evolutionary multiobjective optimization, in: Proceedings of the 3rd Annual Conference on Genetic and Evolutionary Computation, July 2001, pp. 283–290.
[20] K. Deb, H. Jain, An evolutionary many-objective optimization algorithm using reference-point-based nondominated sorting approach, part I: solving problems with box constraints, IEEE Trans. Evol. Comput. 18 (4) (2013) 577–601, https://doi.org/10.1109/tevc.2013.2281535.
[21] H. Ishibuchi, R. Imada, Y. Setoguchi et al., Performance comparison of NSGA-II and NSGA-III on various many-objective test problems. In 2016 IEEE Congress on Evolutionary Computation (CEC). pp. 3045–3052. doi: 10.1109/cec.2016.7744174.
[22] G.C. Ciro, F. Dugardin, F. Yalaoui, et al., A NSGA-II and NSGA-III comparison for solving an open shop scheduling problem with resource constraints, IFAC-PapersOnLine 49 (2016) 1272–1277, https://doi.org/10.1016/j.ifacol.2016.07.690.
[23] V. Yannibelli, E. Pacini, D. Monge, et al., A comparative analysis of NSGA-II and NSGA-III for autoscaling parameter sweep experiments in the cloud, Sci. Program. 6 (2020) 1–17, https://doi.org/10.1155/2020/4653204.
[24] A. Teymourifar, A.M. Rodrigues, J.S. Ferreira, A comparison between NSGA-II and NSGA-III to solve multi-objective sectorization problems based on statistical parameter tuning, in: 2020 24th International Conference on Circuits, Systems, Communications and Computers (CSCC), IEEE, 2020, pp. 64–74, https://doi.org/10.1109/cscc49995.2020.00020.
[25] R. Storn, K. Price, Differential evolution—a simple and efficient heuristic for global optimization over continuous spaces, J. Global Optim. 11 (4) (1997) 341–359, https://doi.org/10.1023/A:1008202821328.
[26] J. Qiang, A Unified Differential Evolution Algorithm for Global Optimization.
[27] F. Ge, K. Li, Y. Han, Solving interval many-objective optimization problems by combination of NSGA-III and a local fruit fly optimization algorithm, Appl. Soft Comput. 114 (2022), 108096, https://doi.org/10.1016/j.asoc.2021.108096.
[28] G. Rudolph, Convergence analysis of canonical genetic algorithms, IEEE Trans. Neural Network. 5 (1) (1994) 96–101, https://doi.org/10.1109/72.265964.
[29] S. Das, P.N. Suganthan, Differential evolution: a survey of the state-of-the-art, IEEE Trans. Evol. Comput. 15 (1) (2010) 4–31, https://doi.org/10.1109/tevc.2010.2059031.
[30] S. Huband, P. Hingston, L. Barone, et al., A review of multiobjective test problems and a scalable test problem toolkit, IEEE Trans. Evol. Comput. 10 (5) (2006) 477–506, https://doi.org/10.1109/tevc.2005.861417.
[31] C. Audet, J. Bigeon, D. Cartier, et al., Performance indicators in multiobjective optimization, Eur. J. Oper. Res. 292 (2) (2021) 397–422, https://doi.org/10.1016/j.ejor.2020.11.016.
[32] W. Zhou, G. Sun, Z. Yang, et al., BP neural network based reconstruction method for radiation field applications, Nucl. Eng. Des. 380 (2021), 111228, https://doi.org/10.1016/j.nucengdes.2021.111228.
[33] M. Ni, C. Lian, S. Zhang, et al., Structural design and preliminary analysis of liquid lead–lithium blanket for China Fusion Engineering Test Reactor, Fusion Eng. Des. 94 (2015) 61–66, https://doi.org/10.1016/j.fusengdes.2015.03.018.
[34] W. Li, W. Shi, Q. Zeng, et al., The assessment of shutdown dose rate and radioactive waste of HCSB during its replacement in CFETR, Fusion Eng. Des. 131 (2018) 15–20, https://doi.org/10.1016/j.fusengdes.2018.04.031.
[35] Z. Lv, H. Chen, C. Chen, et al., Preliminary neutronics design and analysis of helium cooled solid breeder blanket for CFETR, Fusion Eng. Des. 95 (2015) 79–83, https://doi.org/10.1016/j.fusengdes.2015.04.038.
[36] S. Cui, D. Zhang, Y. Lang, et al., A new method for improving the tritium breeding and releasing performance of China Fusion Engineering Test Reactor phase II helium-cooled ceramic breeder blanket, Int. J. Energy Res. 44 (7) (2020) 5977–5989, https://doi.org/10.1002/er.5392.
[37] Y.C. Wu, Multifunctional neutronics calculation methodology and program for nuclear design and radiation safety evaluation, Fusion Sci. Technol. 74 (4) (2018) 321–329, https://doi.org/10.1080/15361055.2018.1475162.
[38] R.A. Forrest, R. Capote, N. Otsuka, et al., FENDL-3 Library-Summary Documentation (No. INDC (NDS)–0628), International Atomic Energy Agency, 2012.
[39] K.L. Lawrence, ANSYS Workbench Tutorial Release 14, SDC publications, 2012.

[40] H. Chen, M. Li, Z. Lv, et al., Conceptual design and analysis of the helium cooled solid breeder blanket for CFETR, Fusion Eng. Des. 96 (2015) 89–94, https://doi.org/10.1016/j.fusengdes.2015.02.045.
[41] M. Moscardini, Helium Cooled Pebble Bed Test Blanket Module for a Nuclear Fusion Reactor: Thermo Mechanical Analyses of the Breeder Unit, 2013.
[42] J. Reimann, S. Hermsmeyer, Thermal conductivity of compressed ceramic breeder pebble beds, Fusion Eng. Des. 61 (2002) 345–351, https://doi.org/10.1016/s0920-3796(02)00165-5.
[43] P. Kittisuwan, Relation between Penalized Least Squares Regression and Bayesian Estimation in AWGN Based on Novel Penalty Function of Pareto Density, ICT Express, 2022, https://doi.org/10.1016/j.icte.2022.01.012.
[44] J. Li, Q. Zeng, M. Chen, J. Jiang, S. Zheng, FDS Team, Comparison analysis of 1D/2D/3D neutronics modeling for a fusion reactor, Fusion Eng. Des. 83 (10–12) (2008) 1678–1682, https://doi.org/10.1016/j.fusengdes.2008.06.051.
[45] J.C. Helton, F.J. Davis, Latin hypercube sampling and the propagation of uncertainty in analyses of complex systems, Reliab. Eng. Syst. Saf. 81 (1) (2003) 23–69, https://doi.org/10.1016/s0951-8320(03)00058-9.
[46] L. El-Guebaly, V. Massaut, K. Tobita, et al., Evaluation of Recent Scenarios for Managing Fusion Activated Materials: Recycling and Clearance, Avoiding Disposal, UWFDM-1333, University of Wisconsin Fusion Technology Institute~ Sep, 2007.